Electronic Supplementary Material (ESI) for Physical Chemistry Chemical Physics

Supporting Information

Self-assembled hollow nanosphere arrays used as low Q whispering gallery mode resonators on thin film solar cells for light trapping

Jun Yin, *Yashu Zang*, *Chuang Yue*, *Xu He*, *Jing Li**, *Zhihao Wu** and *Yanyan Fang*

1. FDTD simulations:

Full-field electromagnetic wave calculations are performed using a commercially available FDTD simulation software package. The permittivity parameters of ZnO materials measured by spectroscopic ellipsometry in previous works were employed in the FDTD simulation with considering the similar experimental situations as those in this work[1]. For other materials used in the simulation, such as ITO, Si_3N_4, c-Si, a-Si and sapphire, the permittivity parameters were taken from the reference[2]. The simulated transmission spectra shown in Figure 2c were directly obtained with a frequency-domain transmission monitor placed in the sapphire substrate of the model. Periodic boundary condition was used on the plane of substrate and perfectly matched layer (PML) conditions boundary was used on the other two sides of the simulation box. Broadband (300-900 nm) plane wave source with normal incidence to the substrate was used. The simulated reflection spectra shown in Figure 2d were also directly obtained by placing the frequency-domain transmission monitor above the substrates and the ZnO HNS arrays. In order to obtain the resonance spectra in the ZnO dielectric 3-D nano-cavity as shown in Figure 3a, a broadband dipole source was placed in the shell layer at the bottom of a typical ZnO HNS with the core diameter of 450 nm and shell thickness of 40 nmand a pulse was sent into this nano-cavity, resulting in different simultaneously excited cavity modes. The resonance spectra intensity was recorded by a point time monitor placed on the other side of the shell layer. To obtain the pattern of each resonance mode, plane wave source with the relevant wavelength at each resonance peak centre was applied in simulation for a single ZnO HNS and the electric field distribution was recorded. The corresponding scattering efficiency (shown in Figure 3c) for a single ZnO HNS

was obtained by a total-field scattered-field method that directly calculated the scattered power by means of frequency-domain transmission monitors positioned in the scattered field region.

The light absorption in the c-Si substrate decorated with these ZnO optical arrays was extracted by the frequency-domain transmission monitor, where the calculation model is schematically shown in Figure 7a. Broadband plane light source (300-1200 nm) weighted against the air mass 1.5 (AM 1.5) solar spectra propagating along the *-z* direction and perfectly matched layer (PML) boundary conditions were used in the incident direction to prevent interference effect. Hexagonally packed ZnO HNS arrays were placed on the bare silicon substrate. Additionally, semi-infinite boundary for silicon substrate and periodic boundary condition for *xy* plane were set as the FDTD region, assuming that any light travelling into the Si substrate would be absorbed, which also agrees well with the actual situation of the c-silicon absorption layer having a considerable thickness. The light absorption for the a-silicon solar cell shown in Figure 8a was obtained from the difference of the two frequency-domain transmission monitor just sandwiched the a-silicon active layer. The number of photons absorbed (*NPA*) in the Si substrate was calculated from the simulation result using the following equation:

$$NPA = \frac{\int \frac{\lambda}{hc} T(\lambda) I_{AM1.5}(\lambda) d\lambda}{\int \frac{\lambda}{hc} I_{AM1.5}(\lambda) d\lambda} \qquad (1)$$

Where λ is the wavelength of light in free space, h is Plank's constant, c is the speed of light in free space, $T(\lambda)$ is the transmittance of light in Si, and $I_{AM1.5}$ is the AM 1.5 solar spectrum(ASTM G173-03). If assuming that all electron-hole pairs contribute to photocurrent, the short circuit current density J_{sh} can be given by

$$J_{sh} = NPA \cdot e \qquad (2)$$

Where e is the charge on an electron.

2. Schematic illustration of the fabrication processes for ZnO HNS arrays.

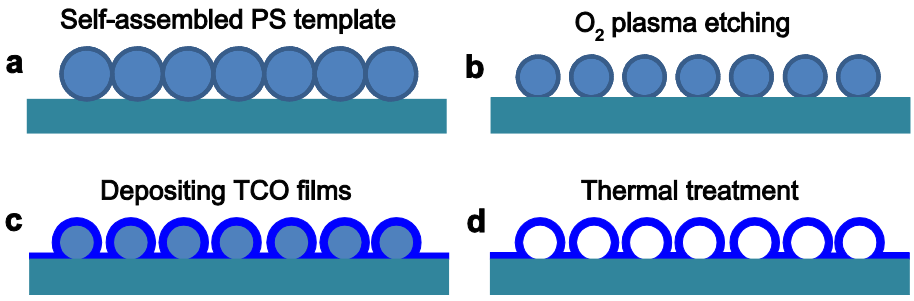

Figure S1. The fabrication processes of ZnO HNS arrays are schematically shown in figure (a)-(d) by using the colloidal template method combined with the film deposition process. Briefly, a self-assembled PS nanosphere monolayer on a silicon substrate was used as the template to prepare ZnO HNS structures by a sputtering deposition process. RIE was introduced to manipulate the size of the PS nanospheres in the template by adjusting the O_2 plasma etching time. After deposition of a thin ZnO film, the PS nanospheres were vaporized by annealing the samples at 500°C for 30 min in ambient N_2. Eventually, ZnO hollow nanospheres were formed on the substrates with an improved crystal quality caused by the heat treatment.

3. Large scale monolayer ZnO HNS arrays.

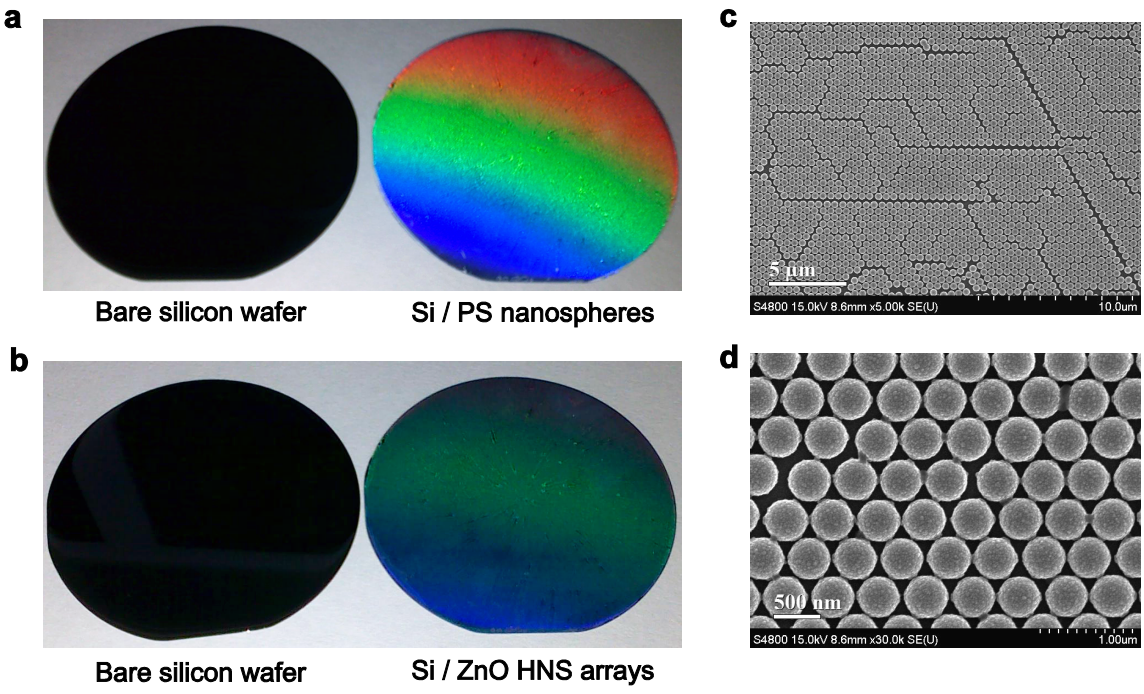

Figure S2. Wafer scale monolayer ZnO HNS arrays can be successfully fabricated using the colloidal PS nanospheres as the template: (a) The photograph of the self-assembled wafer

scale PS nanospheres monolayer on a 2 inch silicon wafer compared with a bare silicon wafer; (b) The photograph of the fabricated monolayer ZnO HNS arrays on the silicon substrate by using the self-assembled monolayer PS nanospheres as the template shown in (a); The SEM images of the as-fabricated ZnO HNS arrays in (c) low and (d) high magnifications. The colloidal sphere template was assembled using the 500 nm PS nanospheres and etched by O_2 plasma for 30 s. The fabricated ZnO HNS arrays have a core diameter D = 400 nm and shell thickness T = 40 nm. Apparent diffraction colour can be seen on the fabricated ZnO HNS arrays on silicon substrate as shown in Fig. S2b, which should come from the elastic coherent scattering from the ZnO HNS arrays and happens at specific angles that satisfies Bragg's equation. The diffraction light can be considered as a specific scattering of light from the particle. As the size of the ZnO hollow spheres is comparable to the wavelength of the incident light, Mie' scattering is the dominant scattering mechanism in this work. Given the supported WGM resonances in the ZnO hollow cavity, a strong scattering efficiency can be obtained in these HNS arrays as described in the paper (Fig. 3c). Light confined in the ZnO HNSs guided as WGM resonance can be easily coupled into the active layer below and travels as guide mode along the active layer. This is the main mechanism for light trapping enhancement in this work.

4. Shell thickness dependence of the resonance peaks in a ZnO HNS nanocavity.

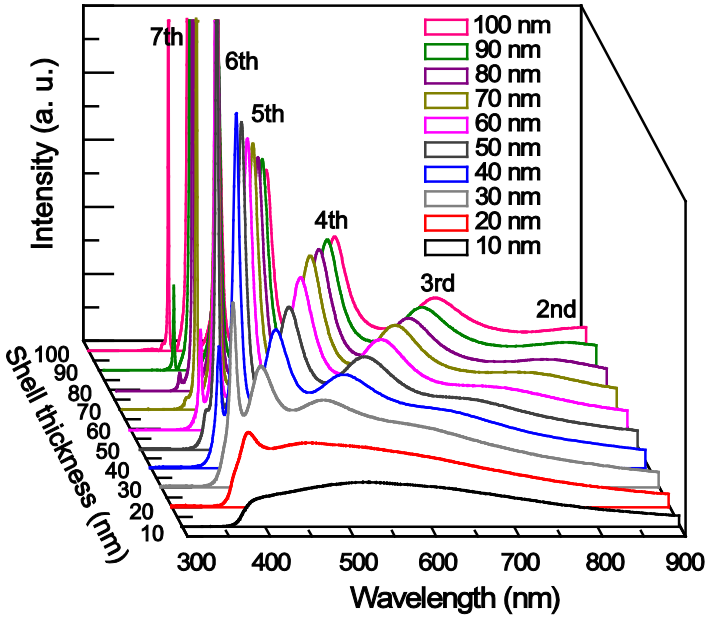

Figure S3. The resonance modes in a ZnO HNS nanocavity as a function of the shell thickness were investigated by FDTD simulations as shown in the figure. The core diameter of ZnO HNS used in the simulation was 450 nm. It can be seen that as the shell thickness increases, a certain resonance mode undergoes a red shift in its peak wavelength and new higher order resonances appear, which are owing to the elongated effective optical path along the shell surface. Higher order of WGM resonance also has a higher quality (Q) factor in the cavity.

5. Calculated short-circuit current density (J_{sc}) on ZnO HNS decorated c-silicon solar cell under AM 1.5 solar spectra.

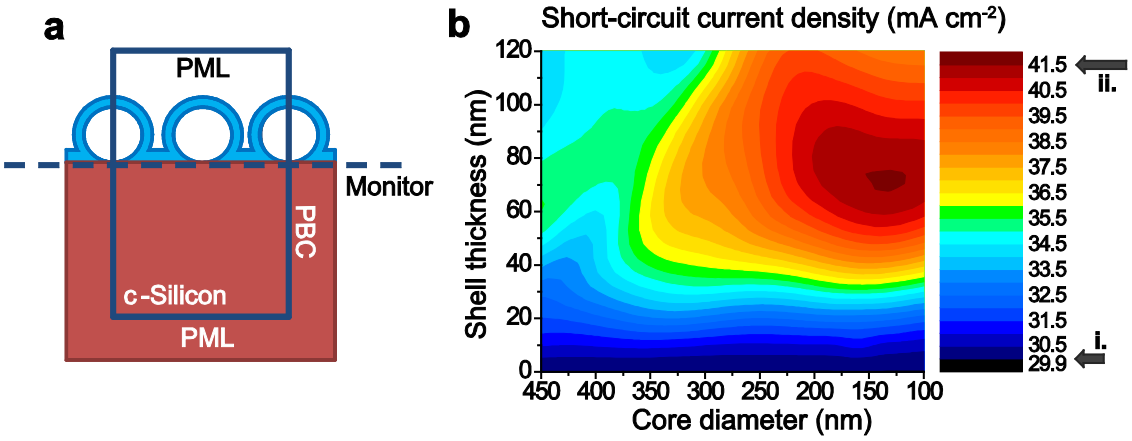

Figure S4 (a) FDTD simulation configuration of the ZnO TCO HNS arrays decorated crystalline silicon solar cell; (b) mapping pattern of the short-circuit current density as the function of the core diameter (D) and shell thickness (T) with the constant period (P = 500 nm). The arrow (i.) shown in (b) refers to the bare silicon solar cell absorption level (29.9 mA cm^{-2}) and arrow (ii.) refers to the SiN ARC modified crystalline silicon solar cell (41.5 mA cm^{-2}).

6. Angle dependent light absorption on the ZnO HNS arrays modified solar cells

The angle dependent light absorption on c-silicon and a-silicon thin film solar cell decorated with ZnO hollow nanosphere (HNS) arrays layer has been investigated and compared with the single AR layer coated cells. Light at higher angles into the crystalline silicon and amorphous silicon thin film solar cell also has been demonstrated for effectively coupling and absorption. Figure S6a shows the simulated absorption in a c-silicon solar cell decorated with

the ZnO HNS arrays on the surface compared with the bare silicon one under AM 1.5 solar spectra at different incident angles. The angle dependent light absorption for a-silicon thin film solar cell also has been simulated as seen in Figure S6b. It can be found that the enhanced absorption on the solar cells via the HNS coupling process exhibits the same tendency as the ARC modified one in which the absorption enhancement decreases as the angle increases. For the thin film solar cell as illustrated in Figure S6b, considerable absorption enhancement still can be maintained even at lager incident angle compared with the optimized AZO anti-reflection layer coated one.

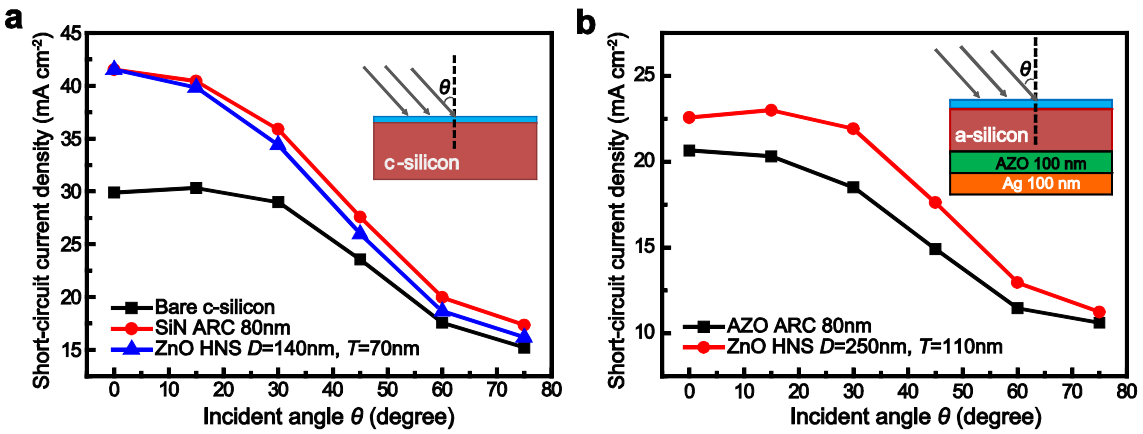

Figure S5 The angle dependent light absorption for (a) c-silicon solar cell decorated with ZnO hollow nanosphere (HNS) arrays layer or single SiN ARC layer compared with bare c-silicon; (b) a-silicon thin film solar cell decorated with ZnO HNS arrays compared with single AZO AR layer coated one.

7. ZnO HNS arrays fabricated on flexible substrates.

The ZnO HNS arrays also has been successfully fabricated on flexible substrates and the samples exhibit good flexibility and stability. Figure S7a shows the ZnO HNS arrays fabricated on the PMMA (Polymethyl methacrylate) substrate by depositing the ZnO film (shell thickness ~60 nm) on PS template followed by the PS core removal by etching in THF (Tetrahydrofuran). As shown in Figure S7b, the transmission spectra remain almost the same after bending the substrate even for twenty times, which also demonstrates the good flexibility and mechanical stability of the ZnO HNS structure. So, it is evident that the hollow

sphere arrays are mechanically stable and could bear other chip fabrication processes for the practical application in a solar cell, including flexible thin film solar cells.

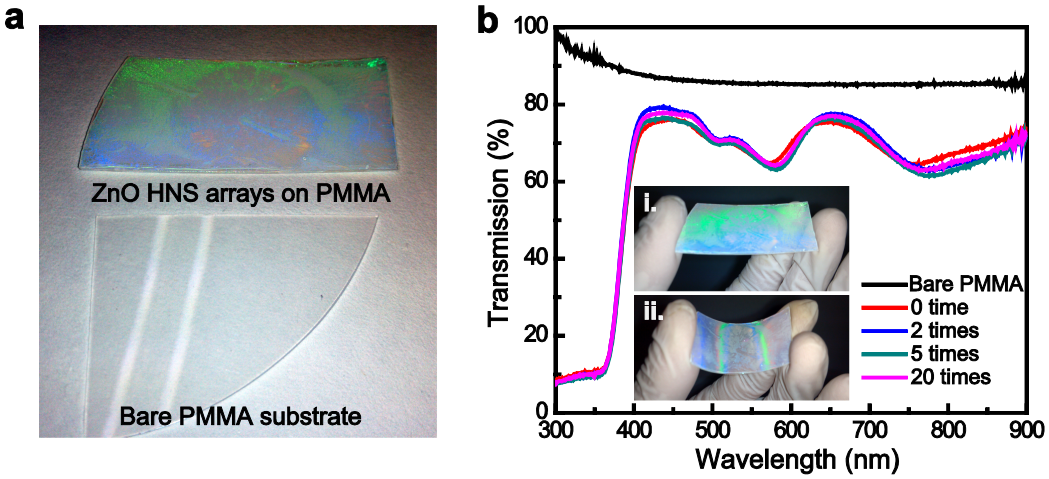

Figure S6 (a) The photograph of the as-fabricated ZnO HNS arrays on PMMA substrate compared with the bare PMMA substrate; (b) the transmission spectra of the sample bended for different times. No obvious changes can be found on the spectra.

References

1. K. Postava, H. Sueki, M. Aoyama, T. Yamaguchi, Ch. Ino, Y. Igasaki, M. Horie. *J. Appl. Phys.*, 2000, **87**, 7820.
2. Palik, E. D. *Handbook of Optical Constants of Solids*, Academic Press, San Diego, USA, **1998**.